JUSTC
Article
http://justc.ustc.edu.cn
Received: April 29, 2024; Accepted: June 14, 2024

# A novel missense mutation in *QRICH2* causes male infertility due to multiple morphological abnormalities of the sperm flagella

Yousaf Raza, Huan Zhang, Muhammad Zubair, Ansar Hussain, Nisar Ahmad, Min Chen, Gang Yang, Musavir Abbas, Tanveer Abbas, Muhammad Shoaib, Ghulam Mustafa, Imtiaz Ali, Meftah Uddin, Suixing Fan, Wasim Shah ✉, and Qinghua Shi ✉

*Center for Reproduction and Genetics, The First Affiliated Hospital of USTC, Division of Life Sciences and Medicine, Biomedical Sciences and Health Laboratory of Anhui Province, Institute of Health and Medicine, Hefei Comprehensive National Science Center, University of Science and Technology of China, Hefei 230027, China*

✉Correspondence: Wasim Shah, E-mail: shah86@ustc.edu.cn; Qinghua Shi, E-mail: qshi@ustc.edu.cn


## Graphical abstract

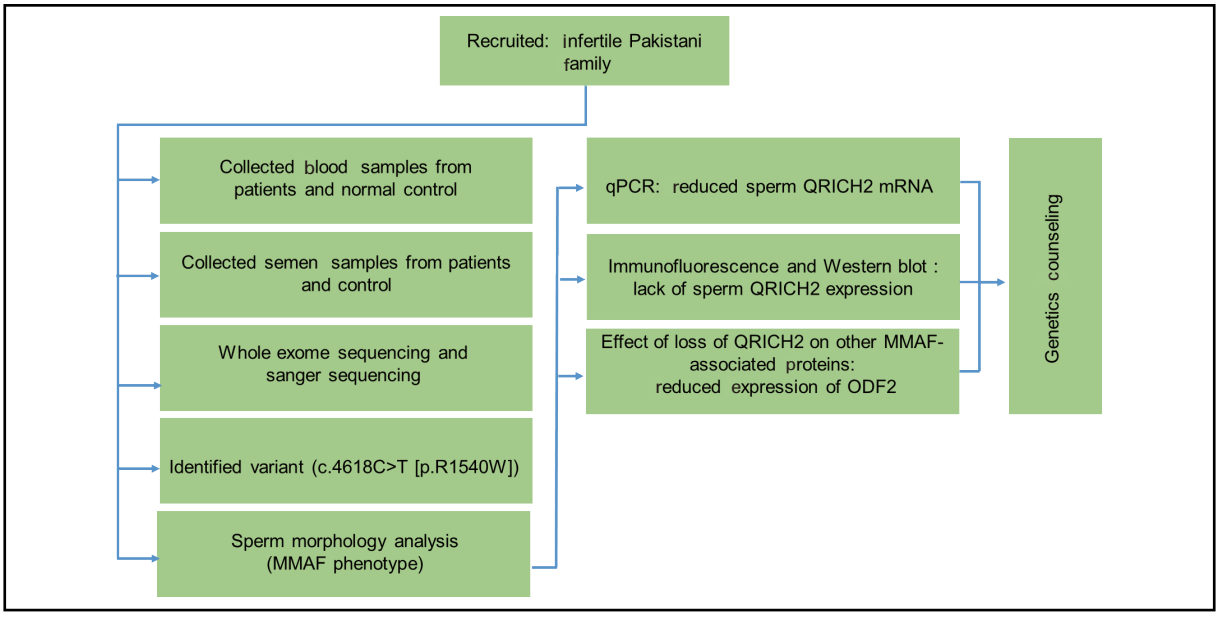


*Loss-of-function mutation in QRICH2 causes MMAF and male infertility.*

## Public summary

- Whole-exome sequencing in a Pakistani consanguineous family identified a new homozygous missense variant (c.4618C>T) in the *QRICH2* gene, pinpointing it as a primary cause of MMAF-associated male infertility. This variant disrupts the function of *QRICH2*, which is crucial for sperm flagellar biogenesis, leading to abnormal sperm morphology.
- Morphological analysis confirmed the MMAF phenotype in affected patients, characterized by bent, irregular, short, or absent sperm flagella.
- Molecular investigations revealed reduced *QRICH2* mRNA expression and the absence of the QRICH2 protein in sperm cells harboring the homozygous mutation. Furthermore, patients presented decreased levels of outer dense fiber 2 (ODF2), suggesting a broader impact on sperm function beyond flagellar development. These findings underscore the genetic underpinnings of MMAF-related infertility and underscore the need for genetic counseling in affected families.

**Citation:** Raza Y, Zhang H, Zubair M, et al. A novel missense mutation in *QRICH2* causes maleinfertility due to multiple morphological abnormalities of the sperm flagella. *JUSTC*, **2024**, 54(9): 0904. CSTR: 32290.14.JUSTC-2024-0064. DOI: 10.52396/JUSTC-2024-0064

JUSTC

Article

http://justc.ustc.edu.cn

Received: April 29, 2024; Accepted: June 14, 2024

# A novel missense mutation in *QRICH2* causes male infertility due to multiple morphological abnormalities of the sperm flagella

Yousaf Raza, Huan Zhang, Muhammad Zubair, Ansar Hussain, Nisar Ahmad, Min Chen, Gang Yang, Musavir Abbas, Tanveer Abbas, Muhammad Shoaib, Ghulam Mustafa, Imtiaz Ali, Meftah Uddin, Suixing Fan, Wasim Shah ✉, and Qinghua Shi ✉

*Center for Reproduction and Genetics, The First Affiliated Hospital of USTC, Division of Life Sciences and Medicine, Biomedical Sciences and Health Laboratory of Anhui Province, Institute of Health and Medicine, Hefei Comprehensive National Science Center, University of Science and Technology of China, Hefei 230027, China*

✉Correspondence: Wasim Shah, E-mail: shah86@ustc.edu.cn; Qinghua Shi, E-mail: qshi@ustc.edu.cn


Cite This: *JUSTC*, **2024**, 54(9): 0904 (9pp)  Read Online  SI Supporting Information

**Abstract:** Multiple morphological abnormalities of the sperm flagella (MMAF) are characterized by bent, irregular, short, coiled, and absent flagella. MMAF is caused by a variety of genes, some of which have been identified. However, the underlying genetic factors responsible for the majority of MMAF cases are still largely unknown. The glutamine-rich 2 (*QRICH2*) gene plays an essential role in the development of sperm flagella by regulating the expression of essential sperm flagellar biogenesis-associated proteins, and genetic variants of *QRICH2* have been identified as the primary cause of MMAF in humans and mice. Here, we recruited a Pakistani consanguineous family to identify the genetic variant causing infertility in patients with MMAF. Whole-exome sequencing and Sanger sequencing were conducted to identify potentially pathogenic variants causing MMAF in infertile patients. Hematoxylin and eosin (HE) staining was performed to analyze sperm morphology. Quantitative polymerase chain reaction, western blot, and immunofluorescence staining analyses were conducted to observe the expression of *QRICH2* in spermatozoa. A novel homozygous missense variant (c.4618C>T) in *QRICH2* was identified in the affected patients. Morphological analysis of spermatozoa revealed the MMAF phenotype in infertile patients. qPCR revealed a significant reduction in the level of sperm *QRICH2* mRNA, and immunofluorescence staining revealed a lack of sperm QRICH2 expression. Additionally, patients harboring a homozygous *QRICH2* mutation presented reduced expression of outer dense fiber 2 (ODF2) in sperm, whereas sperm expression of A-kinase anchor protein 4 (AKAP4) was normal. These findings expand our understanding of the genetic causes of MMAF-associated male infertility and emphasize the importance of genetic counseling.

**Keywords:** male infertility; MMAF; asthenozoospermia; *QRICH2*; missense mutation

**CLC number:** R698$^{+}$.2  **Document code:** A

## 1 Introduction

The occurrence of male infertility in the worldwide population ranges from approximately 9% to 15% according to available surveys of infertility cases[1]. Multiple morphological abnormalities of the sperm flagella are severe forms of sperm defects responsible for asthenoteratozoospermia[2], characterized by morphologically abnormal spermatozoa, including bent, short, irregular, coiled, and absent flagella[3]. The reduced motility of spermatozoa from patients with MMAF is due to ultrastructural defects in sperm flagella. The structure of normal sperm flagella consists of a typical 9+2 axonemal arrangement with nine outer peripheral microtubule doublets (MTDs) encircling a central pair (CP)[4] and with T-shaped structures known as radial spokes that act as connections between the MTDs and the central pair[5]. The 9+2 axonemal structure occurs along the full length of the sperm flagella, which is encircled by outer dense fibers (ODFs) and the mitochondrial sheath at the midpiece and by ODFs and the fibrous sheath at the principal piece[6]. All patients with MMAF exhibited flagellar ultrastructural defects, which included the absence of a central pair and incomplete or disorganized arrangements of MTDs, ODFs, and the fibrous sheath. These ultrastructural defects lead to aberrant sperm motility and male infertility[7–15].

Many genetic factors cause MMAF. In 2014, researchers identified *DNAH1* as the first known gene linked to the MMAF phenotype[16]. To date, more than 40 MMAF-associated genes have been identified, including *AK7, AKAP4, AKAP3, DNAH1, ODF2, SPAG6,* and *QRICH2*[10,17–22], highlighting the diverse genetic heterogeneity of this phenotype. However, the causes of nearly 50% of MMAF cases remain unexplained. Therefore, it is important to identify other potential gene mutations associated with the MMAF pheno-



CSTR: 32290.14.JUSTC-2024-0064
DOI: 10.52396/JUSTC-2024-0064
*JUSTC*, **2024**, 54(9): 0904

type to fully understand the genetic causes underlying this phenotype[6].

Glutamine-rich 2 (*QRICH2)* plays an essential role in the development of sperm flagella by regulating the expression of other flagellar biogenesis-associated proteins. Two homozygous nonsense mutations (c.192G>A [p. L64*] and c.3037C>T [p.R1013*]) in *QRICH2* were reported in unrelated Chinese families, in which the affected individuals presented the MMAF phenotype and infertility. The *Qrich2* knockout mouse model presented morphological and ultrastructural defects similar to those observed in male patients[22]. Another study in North Africa reported two homozygous nonsense variants (c.3501C>G [p.Y1167*] and c.4614C>G [p.Y1538*]) of *QRICH2* in male patients with the MMAF phenotype[23]. A recent report revealed a 1-bp deletion mutation in bovine *QRICH2,* which severely affects sperm concentration and motility and is associated with the MMAF phenotype[24].

Consanguineous marriages, which are common in some populations, including Pakistan, have been shown to increase the risk of inherited disorders because of the increased likelihood of recessive alleles being homozygous in offspring[25]. Whole-exome sequencing (WES) was performed on recruited patients from a Pakistani consanguineous marriage who exhibited the MMAF phenotype, and a homozygous missense mutation (c.4618C>T [p.R1540W]) in *QRICH2*, which cosegregated with infertility in this family, was identified.

## 2 Materials and methods

### 2.1 Ethics statement

This study was approved by the Ethics Committee of the First Affiliated Hospital of the University of Science and Technology of China (USTC) (2019-KY-168). Prior to commencing this study, written informed consent forms were obtained from all individual participants included in this study.

### 2.2 Study subjects and clinical investigation

In this study, a Pakistani consanguineous family (Register number ID: PK-INF-1148) with two infertile male patients (IV:1 & IV:3) diagnosed with asthenozoospermia was recruited. Routine semen analysis was performed on the patients and fertile control samples as per the standard guidelines set by the World Health Organization (WHO)[26]. The semen samples for fertile control were obtained from the volunteers at the First Affiliated Hospital of USTC, University of Science and Technology of China.

### 2.3 Hematoxylin and eosin (H&E) staining

To evaluate sperm morphology, the sample slides were subjected to H&E staining according to the standard guidelines established by the WHO[26]. Briefly, the patient's smear slides were stained with hematoxylin for 25 min and then rinsed in $ddH_2O$ for 1 min. After that, the slides were dipped in 1% HCl and washed with tap water to remove the remaining color of the hematoxylin. The slides were subsequently dehydrated with 50%, 70%, or 80% ethanol for 1 min, stained with eosin for 5 min, and again dehydrated in 100% ethanol for 2 min. After staining, the smear slides were immersed in xylene for 5 min and sealed with coverslips using natural balsam. Morphological analysis was conducted for at least 200 spermatozoa on each of the smear slides of patients under an optical microscope (Nikon, Tokyo, Japan).

### 2.4 WES and variant screening

Genomic DNA was extracted from the peripheral blood cells of the participating family subjects (III:1, III:2, IV:1, IV:2, and IV:3) via the Flexi Gene DNA Kit following the manufacturer's protocol. The extracted DNA from patients IV:1 and IV:3 and their fathers (III:1) was sent for WES via the AIExome Enrichment Kit V1 and HiSeq2000 platforms according to standard protocols. A subsequent step involved mapping the filtered reads onto the human reference genome (hg19) with the assistance of Burrows–Wheeler Alignment software[27]. SAM files extracted from the samples were converted into BAM files via SAM tools (http://samtools.sourceforge.net/). Next, Picard software (http://picard.sourceforge.net/) was used to eliminate PCR duplicates and retain correctly paired reads. The processed files were further analyzed through ANNOVAR[28] and the Genome Analysis Toolkit (GATK)[29] (http://www.broadinstitute.org/gatk/). Next, all the BAM files were realigned via the indel realigner. The GATK Unified Genotyper was employed to identify single-nucleotide variants, small insertions, and deletions within the obtained coding sequence intervals. Variants with recessive inheritance were further screened as previously described. The bioinformatics pipeline used in the filtering process is illustrated in the Supporting information (Table S1). BCFtools was used to check for runs of homozygosity[30]. To calculate the inbreeding coefficients, we utilized runs of homozygosity that were over 1.5 Mb. An in-house script was implemented to perform this task. We also verified the relatedness of family members by employing the Peddy tool[31]. The *QRICH2* genomic sequence was obtained from Ensembl (https://grch37.ensembl.org/index.html) and subjected to multiple sequence alignments via Clustal Omega. The impact of single-nucleotide variants was analyzed via Polyphen-2, CADD, SIFT, and Mutation Taster software. Sanger sequencing was performed via the following primers: *QRICH2* (forward: 5′-TCCCTCTGTTCTGCTCACAC-3′, reverse: 5′-GCCCACACTTTCTCTCACAC-3′; chr17: 29465–29432, 368 bp).

### 2.5 RNA extraction and qPCR

Total RNA was extracted from semen samples from patient IV:1 and a normal fertile control, followed by cDNA synthesis and qPCR, as previously described[32]. To normalize the cycle threshold (Ct) values of the samples, the corresponding Ct values of *ACTB* were used to determine the relative expression level of *QRICH2*. The sequences of the primers used were as follows: *QRICH2*, forward 5′-AAGGTGCAGATCCACTTCGG-3′ and reverse 5′-GTAGGGGTAGGTGAGGGTGT-3′; *ACTB*, forward 5′-AATGAGCTGCGTGTGGCTC-3′ and reverse 5′-TAGCACAGCCTGGATAGCAAC-3′.

### 2.6 Immunofluorescence staining

Spermatozoa from patients IV:1 and IV:3 and a normal control were subjected to immunofluorescence as previously described[32]. In brief, fixed smears were subjected to immunofluorescence staining. Initially, the slides were made permeable by treating them with 1× PBST for 40 min. Next, the


CSTR: 32290.14.JUSTC-2024-0064
DOI: 10.52396/JUSTC-2024-0064
*JUSTC*, **2024**, 54(9): 0904

slides were blocked with 3% skim milk and covered with parafilm for 30 min. Then, the primary antibodies prepared with 3% skim milk supernatant (3% milk centrifuged at 12000 × g for 15 min) were added dropwise to each smear at approximately 35 μL per smear. The smears were then covered with parafilm and incubated overnight at 4 °C. The smears were subsequently washed three times for 10 min each with 1× PBST in a dye vat. The slides were then incubated with secondary antibodies for 1 h at 37 °C. Next, the slides were washed three times with 1× PBST for 10 min and dipped in double-distilled water three times. The smear slides were then dried at room temperature, and coverslips were placed on the slides after applying Vectashield with Hoechst. Microscopic imaging was performed via a Nikon ECLIPSE 80i microscope. The supplementary table (Table S2) contains complete information on the antibodies used for IF staining.

### 2.7 Western blot analysis

Human semen samples stored in TRIzol reagent were used to extract total protein as previously described[33]. The proteins that were extracted were separated via SDS–PAGE and subsequently transferred onto nitrocellulose blotting membranes. These membranes were then blocked with 5% skim milk for 30 min before being incubated with primary antibodies overnight at 4 °C. The following day, the membranes were washed three times with 1× TBST for 10 min each, followed by incubation with secondary antibodies at 37 °C for 1 h. Finally, chemiluminescence was used to develop the blots. Details regarding the antibodies used for western blotting are provided in the supplementary table (Table S2).

### 2.8 Statistical analysis

The statistical analysis in this study utilized a student's *t* test. The results are presented as the mean ± SEM. A significance level of $P < 0.05$ denoted a statistically significant difference, with * indicating $P < 0.05$.

## 3 Results

### 3.1 Clinical characteristics of our patients

This study investigated a consanguineous Pakistani family with two infertile male patients (IV:1 and IV:3) (Fig. 1a). Patients IV:1 (39 years old) and IV:3 (34 years old) had been married for 16 and 14 years, respectively. Despite regular

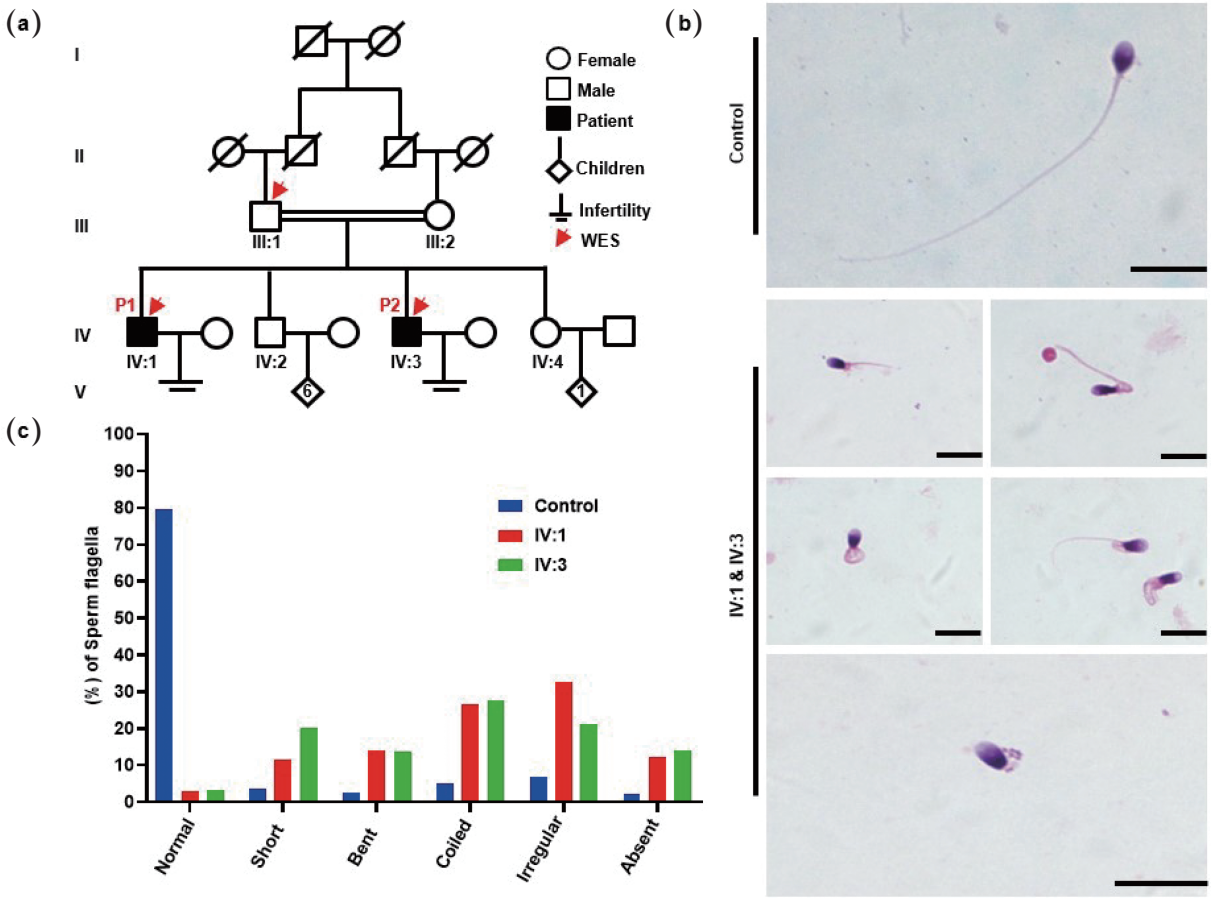


**Fig. 1.** MMAF patients from a Pakistani consanguineous family. (a) Pedigree chart of two infertile male patients, IV:1 and IV:3, from a consanguineous marriage. Squares denote males, while circles represent females. The solid squares denote the patients, and the hollow squares represent the unaffected individuals. The double horizontal lines indicate a consanguineous marriage. The Arabic numerals indicate the number of children born to a couple, whereas the Roman numerals indicate the generation number. The red arrows on the pedigree chart represent individuals analyzed via WES. (b) H&E staining showing the morphological defects of flagella in the spermatozoa of MMAF patients, including (i) short, (ii) bent, (iii) coiled, (iv) irregular caliber, and (v) absent. (c) Statistics of flagellar abnormalities in both the fertile controls and the patients (IV:1 & IV:3). Scale bars = 10 μm. WES: whole-exome sequencing.


CSTR: 32290.14.JUSTC-2024-0064
DOI: 10.52396/JUSTC-2024-0064
*JUSTC*, **2024**, 54(9): 0904

sexual activity, including erection and ejaculation (two to three times per week), their clinically normal wives had not conceived to date. Both patients (IV:1 and IV:3) were normal in height, weight, testicular size, and external genitalia; had no history of exposure to radiation, harmful chemicals, or physical injuries; and did not drink or smoke. Their karyotype (46; XY) was normal, and there were no large-scale deletions in their Y chromosomes. We performed a detailed analysis of the semen phenotype of both patients via light microscopy. Semen analysis revealed that the volume, pH, and sperm concentration of both patients were within the reference range according to WHO guidelines[26]. However, the total motility of spermatozoa decreased to 6.33% ± 1.20% and 2% ± 1% in patients IV:1 and IV:3, respectively, indicating an asthenozoospermic phenotype (Table 1).

Spermatozoa morphology was analyzed via H&E staining. Compared with normal controls, patients IV:1 and IV:3 presented significantly greater percentages of morphologically abnormal spermatozoa (96.03% and 97.43%, respectively) (Fig. 1c). Compared with those of normal sperm, the morphological abnormalities of sperm flagella include coiled, absent, irregular, bent, and short tails. Thus, patients IV:1 and IV:3 were diagnosed with MMAF (Fig. 1b).

**Table 1.** Clinical characteristics of patients carrying the homozygous *QRICH2* missense mutation.

| | IV:1 | IV:3 | Reference values |
|---|---|---|---|
| **Physical examination** [a] | | | |
| Fertility state | Infertile | Infertile | – |
| Age (years old) [b] | 39 | 34 | – |
| Duration of infertility (years) | 16 | 14 | – |
| Height/weight (cm/kg) | 171/85 | 165/82 | – |
| Karyotype analysis | 46, XY | 46, XY | 46, XY |
| Y-chromosome microdeletion | No deletion | No deletion | – |
| **Semen parameters** [c] | | | |
| Semen volume (mL) | 2.33±0.44 | 1.87±0.47 | ≥1.4 |
| Semen pH | Alkaline | Alkaline | Alkaline |
| Sperm concentration ($10^6$/mL) | 20±1.53 | 18.67±1.21 | >16.0 |
| Total motile sperm (%) | 6.33±1.00 | 2.83±0.44 | >42.0 |
| Immotile sperm (%) | 93.67±1.00 | 97.17±0.44 | – |
| **Sperm flagella** [d] | | | |
| Normal (%) | 2.76±0.47 | 3.19±0.45 | >23.0 |
| Short (%) | 11.45±0.81 | 20.13±0.55 | <17.0 |
| Bent (%) | 14.16±0.55 | 13.79±0.22 | <1.0 |
| Coiled (%) | 26.55±0.63 | 27.70±0.71 | <17.0 |
| Irregular (%) | 32.83±0.96 | 21.06±0.57 | <5.0 |
| Absent (%) | 12.25±0.48 | 14.13±1.31 | <2.0 |

[a] Physical examination was performed by a local andrologist.

[b] Age at the time of sampling.

[c] Semen analysis was performed following the WHO guidelines (World Health Organization, 2021).

[d] Three independent experiments were performed. The data are presented as the means ± SEMs.

### 3.2 Identification of a novel missense variant in *QRICH2*

To investigate the genetic factors underlying infertility in this consanguineous Pakistani family, WES was carried out on samples from patients IV:1 and IV:3 and their father (III:1) (Fig. 1a). The analysis strategy used for the WES data is illustrated in Table S1. The WES data underwent several filtration steps to narrow down the disease-causing variants. Variants were excluded (i) if they affected noncoding protein sequences; (ii) if they had an MAF >0.01 in the ExAC, 1000Genomes, or GnomAD; (iii) if the variants were homozygous in our in-house 578 fertile men (283 Europeans, 254 Chinese, and 41 Pakistanis); (iv) if the variants were predicted to be nondeleterious by >50% tools covering them; (v) if the variants were not expressed in the testis; (vi) heterozygous variants were also excluded because MMAF mainly follows the autosomal-recessive inheritance pattern. Following these criteria, four variants in three genes were observed. A literature survey evaluated the genes harboring candidate pathogenic variants from WES. After that, the identified variants were filtered through SpermatogenesisOnline software, and all the variants that had no function in spermatogenesis were omitted. After applying the technical and biological filters mentioned above, we identified a novel homozygous missense variant in *QRICH2* (ENST00000272765.5, c.4618C>T, p.R1540W) associated with MMAF in the family PK-INF-1148. Sanger sequencing was then performed on all the participating family members. This sequencing analysis revealed that the homozygous missense mutation cosegregated with infertility and the MMAF phenotype and was inherited recessively in this family (Fig. 2a). The missense mutation was located in the homozygosity regions of both patients (IV:1 and IV:3) with MMAF (Fig. S1). *QRICH2* is located on chromosome 17 and consists of 19 exons, with a predicted protein structure of 1663 amino acids. The identified mutation was located in exon 15 and encoded the substitution of arginine (R) with tryptophan (W) at position 1540 (Fig. 2b). Multiple sequence alignment revealed that the affected amino acid was conserved across different species (Fig. 2c). The allele frequency of the identified variant was extremely rare in different genome datasets in the 1000 Genomes Project, ExAC Browser, and GnomAD databases. Furthermore, the mutation was identified as potentially damaging by several prediction algorithms, including SIFT, polyphenol-2, and mutation tester. The variant also had a hazard score of 16 in CADD patients, which further supported its possible pathogenicity (Table 2). The I-Mutant and Mutant-Pro tools used to analyze the impact of the loss-of-function mutation on proteins predicted that the missense mutation decreases QRICH2 protein stability (Table S4).

### 3.3 Decreased *QRICH2* mRNA levels in spermatozoa from patient IV:1

To investigate the impact of the homozygous missense mutation on *QRICH2* mRNA levels, q–PCR analysis was performed using spermatozoa RNA from patient IV:1 and a normal control. The results indicated that *QRICH2* mRNA levels were significantly lower in spermatozoa from patient IV:1 than in those from the normal control (Fig. 3a).



CSTR: 32290.14.JUSTC-2024-0064
DOI: 10.52396/JUSTC-2024-0064
*JUSTC*, **2024**, 54(9): 0904

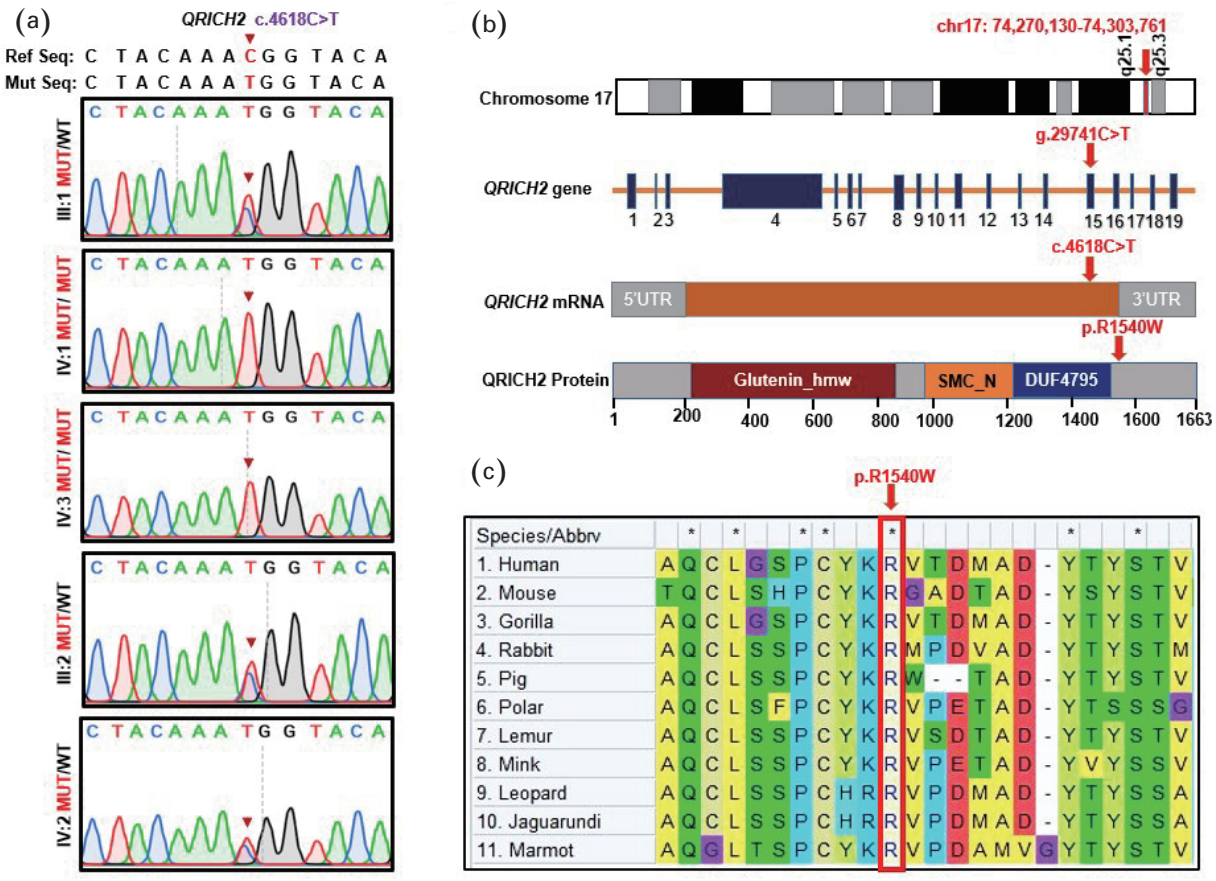


**Fig. 2.** Identification of a novel homozygous *QRICH2* missense variant. (a) Sanger sequencing verification of the *QRICH2* mutation, c.4618C>T, across available family members. The parents (III:1 & III:2) and the fertile brother (IV:2) were heterozygous, whereas the patients (IV:1 & IV:3) were homozygous for the identified mutation. Red arrows indicate the identified mutation. (b) *QRICH2* structure and position of the identified mutation at the genomic, transcriptional, and protein levels. *QRICH2* is located at chromosome 17 and consists of 19 exons encoding a protein of 1663 amino acids (NM_032134.2). The identified mutation is located in exon 15. Red arrows denote the mutation site at the gDNA, CDS, and protein levels. (c) Conservation of the affected amino acid (arginine) across different species is evident in the multiple sequence alignment. MUT: mutant allele; WT: wild-type allele; T: thymine; G: guanine; C: cytosine; A: adenine; *QRICH2*: glutamine-rich protein 2; UTR: untranslated region.

**Table 2.** Pathogenicity of the *QRICH2* variant.

| | | | |
|---|---|---|---|
| ***QRICH2* variant** | | | |
| cDNA alteration | | c.4618C>T | |
| Protein alteration | | p. Arg1540Trp | |
| Variant allele | | homozygous | |
| Variant type | | missense | |
| **Function prediction** | | | |
| Polyphen-2 | | damaging | |
| SIFT | | deleterious | |
| Mutation Taster | | disease-causing | |
| M-CAP | | N/A | |
| CADD | | 16 | |
| **Allele frequency in the human population** | | | |
| Variant | 1000 Genomes Project | Total | 0.0010 |
| | | East Asians | 0 |
| | ExAC Browser | Total | 0.001547 |
| | | East Asians | 0.00112 |
| | GnomAD | Total | 0.002432 |
| | | East Asians | 0 |

NCBI reference sequence number of *QRICH2* GenBank: NM_032134.2.

### 3.4 Loss of the *QRICH2* protein in spermatozoa from patients

To determine the influence of the homozygous mutation on QRICH2 expression, we performed a western blot analysis on sperm lysates extracted from patient IV:1 and a normal control. Western blotting revealed the absence of the QRICH2 band in the sperm protein from patient IV:1, whereas an intact QRICH2 band was observed in the normal control (Fig. 3b). For further validation, we performed immunofluorescence staining on sperm smears from patients IV:1 and IV:3. No QRICH2 signals were detected in spermatozoa from patients IV:1 and IV:3, in contrast to the expression and localization of the QRICH2 protein along the full length of the sperm flagellum observed in the normal control sample (Fig. 3c).

### 3.5 Effects of the loss of QRICH2 on other MMAF-associated proteins

We investigated the effects of the loss of QRICH2 on other flagellar biogenesis-associated proteins, such as ODF2 and AKAP4, via western blot analysis of patient IV:1 and normal control samples. The western blot results revealed a


CSTR: 32290.14.JUSTC-2024-0064
DOI: 10.52396/JUSTC-2024-0064
*JUSTC*, **2024**, 54(9): 0904

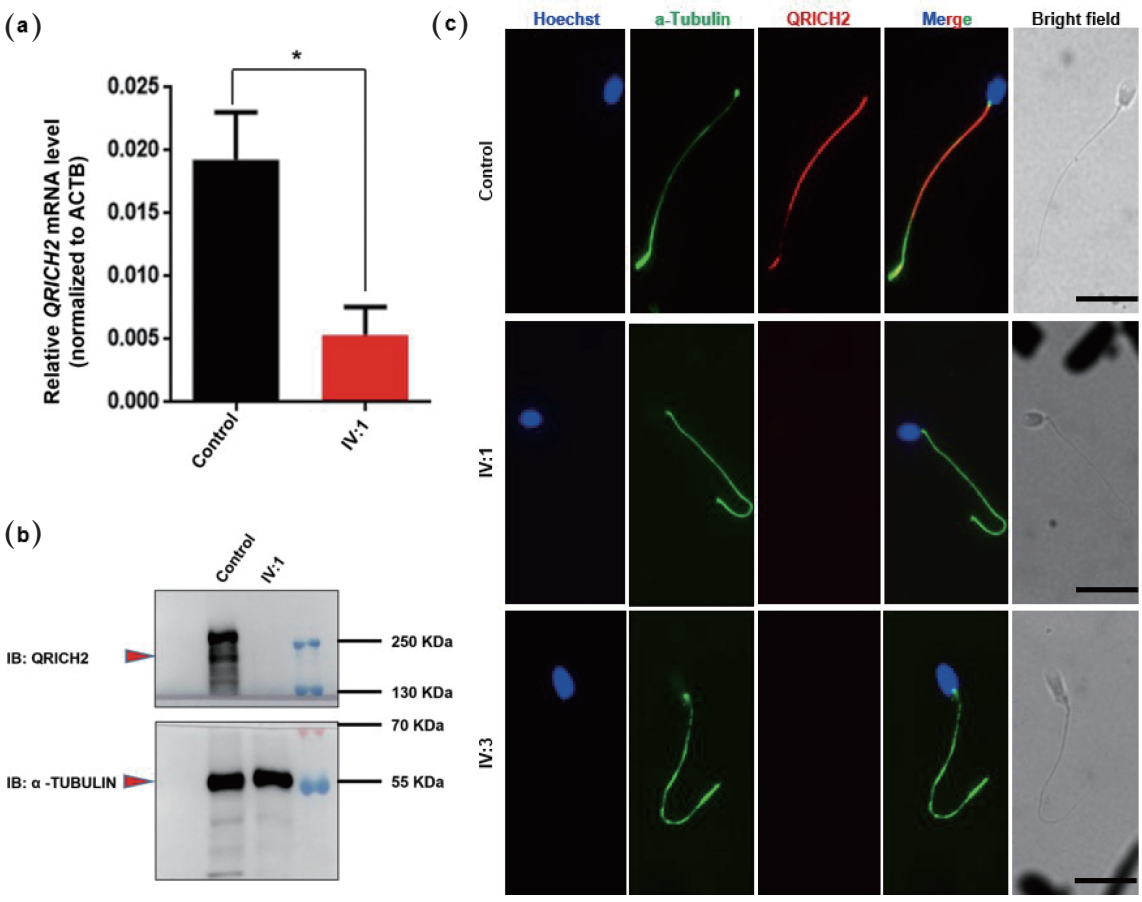


**Fig. 3.** *QRICH2* expression was absent in the patient's spermatozoa. (a) The graph represents the *QRICH2* mRNA expression level of patient IV:1 with a low level of *QRICH2* compared with that of the fertile control. $n = 3$, Student's $t$ test; $^*P < 0.05$. (b) Representative western blot images showing the presence of the QRICH2 band in the sperm lysate of the normal fertile control and the complete absence of the band in patient IV:1. A loading control (e.g., α-tubulin) was used to ensure equal protein loading. (c) Representative images of spermatozoa from normal fertile controls and patients (IV:1 & IV:3) costained with an anti-QRICH2 antibody (red), an anti-α-tubulin antibody (green), and Hoechst (blue, nuclear marker). The QRICH2 signals were absent in the spermatozoa of the patients (IV:1 & IV:3), whereas normal signals of *QRICH2* were observed in the anterior sperm flagella of the normal fertile controls. Scale bars = 10 μm. QRICH2: Glutamine-rich protein 2. Statistical analysis revealed that the difference in *QRICH2* expression between patients (IV:1) and normal fertile controls was significant ($^*P<0.05$).

significantly reduced band for ODF2 and an intact band of AKAP4 in patient IV:1 sperm lysate compared with normal control lysate (Fig. 4a, c). To further validate these results, immunofluorescence staining was conducted on sperm smears from patients IV:1 and IV:3 and a normal control. The immunofluorescence results revealed reduced signals for ODF2 on the midpiece of spermatozoa from patients IV:1 and IV:3 compared with the normal control (Fig. 4b). Normal signals of AKAP4 were observed in spermatozoa from patients IV:1 and IV:3 (Fig. 4d).

## 4 Discussion

In this study, WES screening revealed a novel homozygous missense mutation in *QRICH2* (c.4618C>T, p.R1540W) in a Pakistani consanguineous family that exhibited male infertility with the MMAF phenotype. This mutation was further validated by Sanger sequencing and was found to recessively cosegregate with male infertility in the participating family members. Semen analysis revealed that both affected infertile male patients had reduced sperm motility with the MMAF phenotype. The *QRICH2* variant was found to be conserved across various species and showed a high probability of being pathogenic, according to multiple sequence alignment and in silico prediction tools.

This study demonstrated that a novel missense mutation in *QRICH2* is pathogenic in individuals exhibiting the MMAF phenotype and plays an essential role in human spermiogenesis. QRICH2 regulates the expression of various proteins involved in the formation of sperm flagella, including ODF2, AKAP3, TSSK4, ROPN1, and CABYR. The abnormal development of sperm flagella is caused by mutations in *QRICH2* in affected individuals. Previously, two homozygous nonsense mutations in *QRICH2* were shown to cause the loss of the QRICH2 protein in the spermatozoa of patients diagnosed with MMAF (Table S3). The ultrastructural study of associated spermatozoa revealed severe flagellar ultrastructural defects, including the loss of central pairs, disorganized MTDs, and ODFs. Similar findings were observed in *Qrich2* knockout mice generated through CRISPR/Cas9 technology. These findings indicate the essential role of *QRICH2* in the development of sperm flagella[22]. Another study identified two novel nonsense mutations in *QRICH2* in two unrelated


CSTR: 32290.14.JUSTC-2024-0064
DOI: 10.52396/JUSTC-2024-0064
*JUSTC*, **2024**, 54(9): 0904

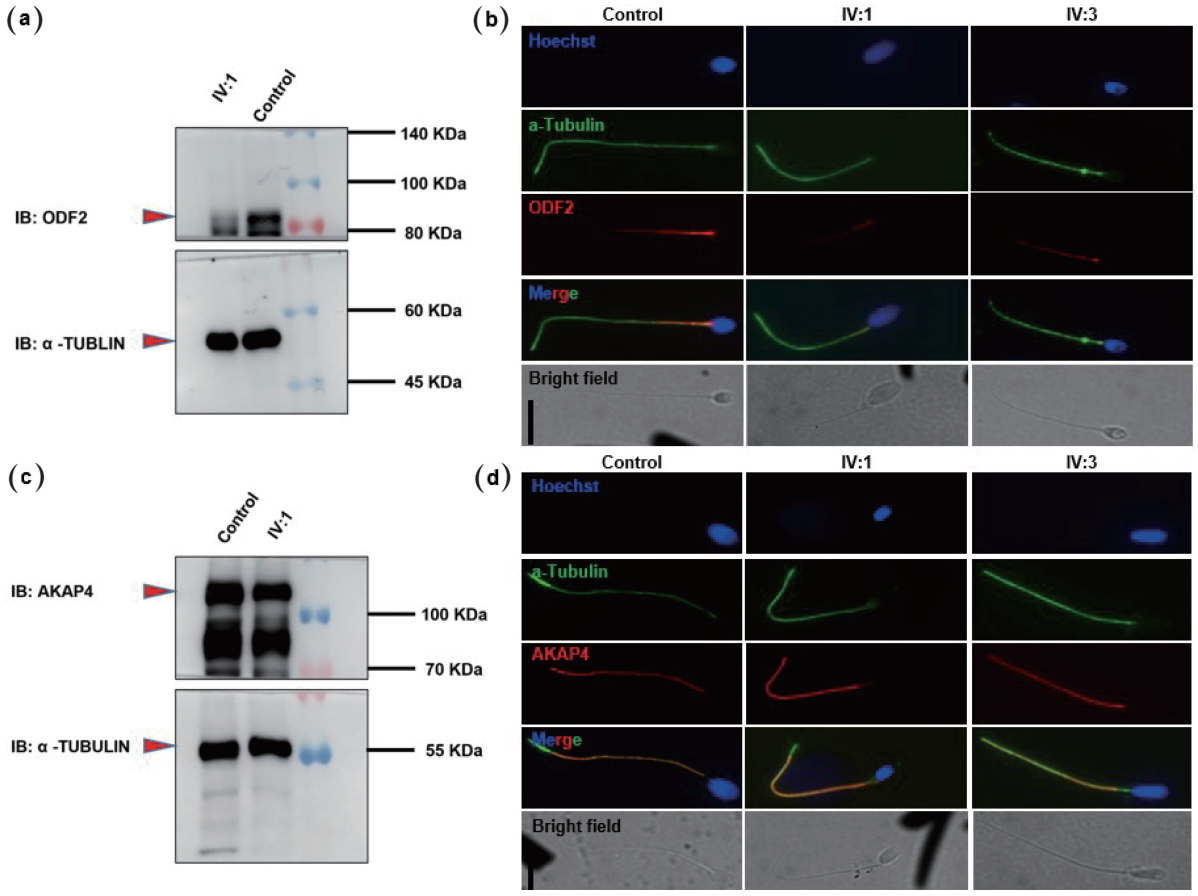


**Fig. 4.** Patients with the *QRICH2* mutation presented reduced ODF2 and normal AKAP4 expression in their spermatozoa. Western blot analysis revealed the presence of a weak band of ODF2 (a) and an intact band of AKAP4 (c) in the sperm lysate of patient IV:1. Spermatozoa from normal fertile controls and patients (IV:1 & IV:3) were costained with anti-ODF2 and anti-AKAP4 antibodies. Images (b) and (d) show the corresponding fluorescence microscopy images of spermatozoa stained with anti-ODF2 and anti-AKAP4 antibodies, an anti-α-tubulin antibody (green), and Hoechst (a nuclear marker). The signals of ODF2 were weak (b), whereas normal signals of AKAP4 were detected in the spermatozoa of the patients (IV:1 & IV:3) (d). Scale bars = 10 μm. QRICH2: Glutamine-rich protein 2. ODF2: Outer dense fiber of sperm tails 2. AKAP4: A-kinase anchoring protein 4.

families from North Africa. Both mutations cause severely impaired motility of spermatozoa in patients with MMAF[23]. The current study revealed a novel homozygous missense mutation in *QRICH2* that causes male infertility with MMAF, thereby expanding the knowledge of the prevalence and spectrum of *QRICH2* variants.

A previous study revealed that *QRICH2* regulates the expression of ODF2 by acting as a trans-regulating factor, and *Qrich2* knockout mice presented reduced expression of ODF2 in spermatozoa[22]. Our current study results were consistent with the reduced expression of ODF2 in the spermatozoa of male patients with disrupted *QRICH2*. Overall, these results indicate that *QRICH2* plays an essential role in the normal expression of ODF2.

AKAP4 is an important protein involved in the formation of the fibrous sheath of sperm flagella. A recent study identified a hemizygous missense variant (c.1285C>T [p.R429C]) in *AKAP4* in three male patients diagnosed with male infertility and MMAF. The decreased AKAP4 expression in the spermatozoa of male patients was associated with a dysplastic fibrous sheath, impaired sperm motility, and infertility. Furthermore, AKAP4 was found to regulate the expression of QRICH2. Reduced expression of AKAP4 induced by a hemizygous missense mutation (c.1285C>T [p.R429C]) reduces the expression levels of *QRICH2* in spermatozoa[6]. Our study revealed that the loss of *QRICH2* does not influence the expression or localization of AKAP4, as evidenced by immunofluorescence and western blot analyses. This finding further suggests that AKAP4 acts upstream to regulate the expression of *QRICH2*[6]. However, further mechanistic studies are needed to elucidate the intricate regulatory pathways underlying the interaction between AKAP4 and QRICH2 in sperm flagellar formation and male fertility. Furthermore, our study focused on a Pakistani consanguineous family, which limits the generalizability of our findings to other populations. Therefore, further studies with diverse ethnic backgrounds and larger sample sizes are needed to validate these results across different populations. We recognize that genetic heterogeneity plays a significant role in MMAF. Future research should aim to identify additional genes and variants that may contribute to the phenotype, particularly given that a substantial proportion of MMAF cases remain genetically unexplained.

## 5 Conclusions

In conclusion, the present study identified a novel homozygous


CSTR: 32290.14.JUSTC-2024-0064
DOI: 10.52396/JUSTC-2024-0064
*JUSTC*, **2024**, 54(9): 0904

missense variant in *QRICH2* that causes male infertility with the MMAF phenotype in two patients recruited from a consanguineous Pakistani family. Our study provides new insights into the regulatory role of *QRICH2* in sperm flagellar biogenesis. Further investigations are needed to explore the interaction of QRICH2 with other flagellar proteins, including those of the central pair and MTDs, which are significantly defective in patients with *QRICH2* mutations. Our findings shed more light on the genetic basis of MMAF and emphasize the importance of genetic counseling and diagnosis for affected men. Furthermore, intracytoplasmic sperm injection (ICSI) is a suggested solution for patients with severe asthenozoospermia associated with MMAF to conceive with a female partner.

## Supporting information

The supporting information for this article can be found online at https://doi.org/10.52396/JUSTC-2024-0064. The supporting information consists of 1 figure and 4 tables.

## Acknowledgements

This work was supported by the National Key Research and Development Program of China (2021YFC2700202, 2022YFA0806303 and 2022YFC2702601), the Global Select Project of the Institute of Health and Medicine, Hefei Comprehensive National Science Center (DJK-LX-2022010), USTC Research Funds of the Double First-Class Initiative (the Joint Fund for New Medicine of USTC) (YD9100002034), and the Fundamental Research Funds for the Central Universities (WK9100000004). We express our gratitude to all the individuals who participated in this study for their valuable cooperation. We thank the Bioinformatics Center of the University of Science and Technology of China, School of Life Sciences, for providing supercomputing resources.

## Conflict of interest

The authors declare that they have no conflict of interest.

## Biographies

**Yousaf Raza** is currently pursuing a master's degree in the Division of Life Sciences and Medicine, University of Science and Technology of China, under the supervision of Prof. Qinghua Shi. His research mainly focuses on male infertility.

**Wasim Shah** is currently engaged as a postdoctoral researcher in the Molecular and Cell Genetics Laboratory of the University of Science and Technology of China. He received his Ph.D degree in Genetics from the University of Science and Technology of China in 2021. His research mainly focuses on the genetic mechanism of male infertility.

**Qinghua Shi** is a Principal Investigator and Professor in Genetics and Cell Biology at Hefei National Research Center for Physical Sciences at the Microscale, and the Division of Life Sciences and Medicine, University of Science and Technology of China. His research interests include molecular regulation of gametogenesis in humans and mammals, identification of mutations causing human infertility, molecular bases and mechanisms of meiosis, and the generation and fates of aneuploid cells.

## References

[1] Barratt C L R, Björndahl L, De Jonge C J, et al. The diagnosis of male infertility: an analysis of the evidence to support the development of global WHO guidance —challenges and future research opportunities. *Human Reproduction Update*, **2017**, *23* (6): 660–680.

[2] Ma Y J, Wu B B, Chen Y H, et al. CCDC146 is required for sperm flagellum biogenesis and male fertility in mice. *Cellular and Molecular Life Sciences*, **2024**, *81*: 1.

[3] Long S H, Fu L L, Ma J, et al. Novel biallelic variants in DNAH1 cause multiple morphological abnormalities of sperm flagella with favorable outcomes of fertility after ICSI in Han Chinese males. *Andrology*, **2024**, *12* (2): 349–364.

[4] Zhang B B, Khan I, Liu C Y, et al. Novel loss-of-function variants in DNAH17 cause multiple morphological abnormalities of the sperm flagella in humans and mice. *Clinical Genetics*, **2021**, *99* (1): 176–186.

[5] Meng X M, Xu C, Li J W, et al. Multi-scale structures of the mammalian radial spoke and divergence of axonemal complexes in ependymal cilia. *Nature Communications*, **2024**, *15*: 362.

[6] Zhang G H, Li D Y, Tu C F, et al. Loss-of-function missense variant of *AKAP4* induced male infertility through reduced interaction with QRICH2 during sperm flagella development. *Human Molecular Genetics*, **2022**, *31* (2): 219–231.

[7] Visser L, Westerveld G H, Xie F, et al. A comprehensive gene mutation screen in men with asthenozoospermia. *Fertility and Sterility*, **2011**, *95* (3): 1020–1024.e9.

[8] Wu B B, Yu X C, Liu C, et al. Essential role of CFAP53 in sperm flagellum biogenesis. *Frontiers in Cell and Developmental Biology*, **2021**, *9*: 676910.

[9] Xu K B, Yang L L, Zhang L, et al. Lack of AKAP3 disrupts integrity of the subcellular structure and proteome of mouse sperm and causes male sterility. *Development*, **2020**, *147* (2): dev181057.

[10] Xu C, Tang D D, Shao Z M, et al. Homozygous SPAG6 variants can induce nonsyndromic asthenoteratozoospermia with severe MMAF. *Reproductive Biology and Endocrinology*, **2022**, *20*: 41.

[11] Xu Y J, Yang B Y, Lei C, et al. Novel compound heterozygous variants in CCDC40 associated with primary ciliary dyskinesia and multiple morphological abnormalities of the sperm flagella. *Pharmacogenomics and Personalized Medicine*, **2022**, *15*: 341–350.

[12] Yin Y Y, Mu W Y, Yu X C, et al. LRRC46 accumulates at the midpiece of sperm flagella and is essential for spermiogenesis and male fertility in mouse. *International Journal of Molecular Sciences*, **2022**, *23* (15): 8525.

[13] Zhang J T, He X J, Wu H, et al. Loss of DRC1 function leads to multiple morphological abnormalities of the sperm flagella and male infertility in human and mouse. *Human Molecular Genetics*, **2021**, *30* (21): 1996–2011.

[14] Zhang R D, Wu B B, Liu C, et al. CCDC38 is required for sperm flagellum biogenesis and male fertility in mice. *Development*, **2022**, *149* (11): dev200516.

[15] Ito C, Akutsu H, Yao R, et al. *Odf2* haploinsufficiency causes a new type of decapitated and decaudated spermatozoa, Odf2-DDS, in mice. *Scientific Reports*, **2019**, *9*: 14249.

[16] Khelifa M B, Coutton C, Zouari R, et al. Mutations in DNAH1, which encodes an inner arm heavy chain dynein, lead to male infertility from multiple morphological abnormalities of the sperm flagella. *The American Journal of Human Genetics*, **2014**, *94* (1): 95–104.

[17] Chang T L, Tang H Y, Zhou X, et al. A novel homozygous nonsense variant of AK7 is associated with multiple morphological abnormalities of the sperm flagella. *Reproductive Biomedicine Online*, **2024**, *48* (5): 103765.

[18] Gu L J, Liu X M, Yang J, et al. A new hemizygous missense mutation, c.454T>C (p.S152P), in *AKAP4* gene is associated with



CSTR: 32290.14.JUSTC-2024-0064
DOI: 10.52396/JUSTC-2024-0064
*JUSTC*, **2024**, 54(9): 0904

asthenozoospermia. *Molecular Reproduction and Development*, **2021**, *88* (9): 587–597.
[19] Liu C Y, Shen Y, Tang S Y, et al. Homozygous variants in AKAP3 induce asthenoteratozoospermia and male infertility. *Journal of Medical Genetics*, **2023**, *60* (2): 137–143.
[20] Wang M, Yang Q Y, Zhou J P, et al. Novel compound heterozygous mutations in DNAH1 cause primary infertility in Han Chinese males with multiple morphological abnormalities of the sperm flagella. *Asian Journal of Andrology*, **2023**, *25* (4): 512–519.
[21] Zhu Z J, Wang Y Z, Wang X B, et al. Novel mutation in ODF2 causes multiple morphological abnormalities of the sperm flagella in an infertile male. *Asian Journal of Andrology*, **2022**, *24* (5): 463–472.
[22] Shen Y, Zhang F, Li F P, et al. Loss-of-function mutations in *QRICH2* cause male infertility with multiple morphological abnormalities of the sperm flagella. *Nature Communications*, **2019**, *10*: 433.
[23] Kherraf Z E, Cazin C, Coutton C, et al. Whole exome sequencing of men with multiple morphological abnormalities of the sperm flagella reveals novel homozygous *QRICH2* mutations. *Clinical Genetics*, **2019**, *96* (5): 394–401.
[24] Hiltpold M, Janett F, Mapel X M, et al. A 1-bp deletion in bovine *QRICH2* causes low sperm count and immotile sperm with multiple morphological abnormalities. *Genetics Selection Evolution*, **2022**, *54*: 18.
[25] Ullah M A, Husseni A M, Mahmood S U. Consanguineous marriages and their detrimental outcomes in Pakistan: an urgent need for appropriate measures. *International Journal of Community Medicine and Public Health*, **2017**, *5* (1): 1–3.
[26] Björndahl L, Brown J K. The sixth edition of the WHO Laboratory Manual for the Examination and Processing of Human Semen: ensuring quality and standardization in basic examination of human ejaculates. *Fertility and Sterility*, **2022**, *117* (2): 246–251.
[27] Li H, Durbin R. Fast and accurate short read alignment with Burrows–Wheeler transform. *Bioinformatics*, **2009**, *25* (14): 1754–1760.
[28] Wang K, Li M Y, Hakonarson H. ANNOVAR: functional annotation of genetic variants from high-throughput sequencing data. *Nucleic Acids Research*, **2010**, *38* (16): e164.
[29] McKenna A, Hanna M, Banks E, et al. The Genome Analysis Toolkit: a MapReduce framework for analyzing next-generation DNA sequencing data. *Genome Research*, **2010**, *20* (9): 1297–1303.
[30] Quinodoz M, Peter V G, Bedoni N, et al. AutoMap is a high performance homozygosity mapping tool using next-generation sequencing data. *Nature Communications*, **2021**, *12*: 518.
[31] Pedersen B S, Quinlan A R. Who's who? Detecting and resolving sample anomalies in human DNA sequencing studies with *peddy*. *The American Journal of Human Genetics*, **2017**, *100* (3): 406–413.
[32] Zhang B B, Ma H, Khan T, et al. A DNAH17 missense variant causes flagella destabilization and asthenozoospermia. *Journal of Experimental Medicine*, **2020**, *217* (2): e20182365.
[33] Ma A, Zeb A, Ali I, et al. Biallelic variants in CFAP61 cause multiple morphological abnormalities of the flagella and male infertility. *Frontiers in Cell and Developmental Biology*, **2022**, *9*: 803818.

(Continued from page 0901–5)

[12] Hou L X, Cui X P, Guan B, et al. Synthesis of a monolayer fullerene network. *Nature*, **2022**, *606*: 507–510.
[13] Okada S, Saito S, Oshiyama A. New metallic crystalline carbon: Three dimensionally polymerized $C_{60}$ fullerite. *Physical Review Letters*, **1999**, *83* (10): 1986.
[14] Pan F, Ni K, Xu T, et al. Long-range ordered porous carbons produced from $C_{60}$. *Nature*, **2023**, *614*: 95–101.
[15] Meng R L, Ramirez D, Jiang X, et al. Growth of large, defect-free pure $C_{60}$ single crystals. *Applied Physics Letters*, **1991**, *59*: 3402–3403.
[16] Sundqvist B. Fullerenes under high pressures. *Advances in Physics*, **1999**, *48* (1): 1–134.
[17] Porezag D, Pederson M R, Frauenheim T, et al. Structure, stability, and vibrational properties of polymerized $C_{60}$. *Physical Review B*, **1995**, *52* (20): 14963.
[18] Haddon R C, Hebard A F, Rosseinsky M J, et al. Conducting films of $C_{60}$ and $C_{70}$ by alkali-metal doping. *Nature*, **1991**, *350*: 320–322.
[19] Wågberg T, Sundqvist B. Raman study of the two-dimensional polymers $Na_4C_{60}$ and tetragonal $C_{60}$. *Physical Review B*, **2002**, *65* (15): 155421.
[20] Kotyczka-Morańska M. Semi-quantitative and multivariate analysis of the thermal degradation of carbon-oxygen double bonds in biomass. *Journal of the Energy Institute*, **2019**, *92* (4): 923–932.
[21] Chowdhury A K M S, Cameron D C, Hashmi M S J. Bonding structure in carbon nitride films: variation with nitrogen content and annealing temperature. *Surface and Coatings Technology*, **1999**, *112*: 133–139.
[22] Lu Y, Zhao C Z, Zhang R, et al. The carrier transition from Li atoms to Li vacancies in solid-state lithium alloy anodes. *Science Advances*, **2021**, *7* (38): eabi5520.
[23] Wang B, Xiao S F, Gan X L, et al. Diffusion properties of liquid lithium-lead alloys from atomistic simulation. *Computational Materials Science*, **2014**, *93*: 74–80.
[24] Jungblut B, Hoinkis E. Diffusion of lithium in highly oriented pyrolytic graphite at low concentrations and high temperatures. *Physical Review B*, **1989**, *40* (16): 10810.



CSTR: 32290.14.JUSTC-2024-0064
DOI: 10.52396/JUSTC-2024-0064
*JUSTC*, **2024**, 54(9): 0904